Adsorption of aluminum on β-SiC(100) surfaces

Lu Wenchang, Zhang Kaiming, and Xie Xide
China Center of Advanced Science and Technology (World Laboratory), P.O. Box 8730, Beijing, People's Republic of China
*and Physics Department, Fudan University, Shanghai 200433, People's Republic of China**
(Received 13 November 1991)

Adsorption properties of Al on β-SiC(100) surfaces are studied by using the extended Hückel theory. The Al/β-SiC(100) interface is sharp and the Al-SiC interaction is limited to a narrow region at the interface. The adsorption of Al on the Si-terminated (100) surface hardly affects the Si-C bond, whereas the adsorption of Al on the C-terminated (100) surface weakens the Si-C bond. Moreover, the Al-Si interaction is weaker than the Al-C interaction. Our results agree qualitatively with experimental observation.

I. INTRODUCTION

The understanding of metal-semiconductor contacts and interfaces is very important in the design and processing of electronic devices. β-SiC is a good candidate for devices used in a high-temperature and -radiation environment and Al is used both in forming contacts on SiC devices[1,2] and as a matrix material in SiC fiber-reinforced composites.[3] Therefore, both experimental and theoretical studies of contacts and interfaces between SiC and aluminum are of great scientific and technological interest.

Mizokawa, Geib, and Wilmsen[4] and Parrill and Chung[5] have investigated the Au/SiC interface and found the Au-Si interaction to be stronger than the Au-C interaction. There are also a number of experimental works on the interface between SiC and other metals, such as Fe,[6,7] Ni,[8,9] Pd,[9,10] and Ti.[11,12]

Using x-ray photoemission spectroscopy (XPS), low-energy electron diffraction (LEED), energy loss spectroscopy (ELS), Bermudez[13,14] has studied the structures of aluminum films on β-SiC(100) and α-SiC(0001) surfaces. It has been shown that the Al-Si interaction is limited to a narrow region at the interface and that the thermally driven Al carbide formation is less favorable for Al on the Si-terminated β-SiC(100) surface than on a C-rich surface. Moreover, he also found that the first two or three monolayers of Al do not exhibit macroscopic metallic behavior and that there is no evidence for pronounced interdiffusion of Si or C with Al either during the deposition of films up to 75 Å thick on a room-temperature substrate or during the annealing of 9-Å-thick films up to 1050 °C. Whereas Porte,[3] using x-ray and ultraviolet photoelectron spectroscopies, has found that Al can penetrate into the bulk α-SiC during annealing beyond 600 °C, Daimon *et al.*[1] have studied the Al/β-SiC contact and found that the diffusion of Al into an *n*-type β-SiC layer induced by annealing at high temperature (900 °C) should cause the formation of a *p*-type layer. In the present paper, theoretical studies of the electronic structure of the Al/β-SiC interface are presented for explaining the sharpness and width of the interface, and a comparison with existing experimental data is made.

To date, not many theoretical investigations have focused on the interfaces between SiC and metals. The electronic structures of Ti/β-SiC (Ref. 15) and Ti, Cu, Pd/α-SiC (Ref. 16) interfaces have been studied using the atom superposition and electronic delocalization molecular-orbital method and the cluster model. Using charge self-consistent extended Hückel theory (EHT),[17] we have studied the adsorption properties of Au on the β-SiC(111) surface[18] and the results obtained agree qualitatively with experiments.[4,5] Here, the same method is adopted to study the adsorption of Al on β-SiC(100) surfaces. Furthermore, an energy-band calculation is carried out for higher Al coverage by using a slab model.

II. CALCULATION METHOD AND PARAMETERS

For a cluster model, in which a molecular-orbital calculation is carried out, the secular equation is given by

$$\sum_{\mu}(H_{\mu\nu}-E_i S_{\mu\nu})C_{\mu i}=0 , \tag{1}$$

where $S_{\mu\nu}$ is overlapping integral between the μth and νth orbitals, which are chosen to be Slater-type orbitals. Within the framework of the charge self-consistent extended Hückel approximation,[17] it is assumed that

$$H_{\mu\mu}=-(I_\mu+\alpha\Delta Q) ; \tag{2}$$

$$H_{\mu\nu}=K\frac{H_{\mu\mu}+H_{\nu\nu}}{2}S_{\mu\nu}, \quad \mu\neq\nu ; \tag{3}$$

where I_μ is ionization potential, K is a parameter suitably chosen, and α is the convergence parameter. ΔQ is charge variation of the atom A:

$$\Delta Q=\sum_i\sum_{\mu,\nu} n_i C_{i\mu}S_{\mu\nu}C_{i\nu}-Q_0 , \tag{4}$$

where n_i is the electronic occupation number of the ith energy level, the summation of μ and ν is taken for all orbitals of the atom A, and Q_0 is the original charge of the atom A. Since ΔQ depends on the wave function $C_{i\nu}$, the calculation is carried out self-consistently.

TABLE I. Orbital exponents ζ (Ref. 22) and ionization energies I (Ref. 23) and parameters K of Si and C atoms.

Orbitals	Si 3s	Si 3p	C 2s	C 2p
ζ	1.6344	1.4284	1.6083	1.5679
I (eV)	13.45	8.15	16.58	11.26
K	1.25	1.65	1.30	1.70

The parameters used in the present calculation are listed in Table I. The parameters K of Si and C are determined by fitting the energy band of bulk β-SiC (Ref. 19) with the experimental results[20] and first-principles calculations.[21]

III. RESULTS AND DISCUSSION

At low coverage, since the adsorbate-adsorbate interaction can be neglected, it is reasonable to use the cluster model and single-atom adsorption for describing the metal-semiconductor system. At higher coverages, where the adsorbate-adsorbate interaction becomes more significant, the band calculation or larger cluster should be used.

A. Low-coverage adsorption

For low-coverage adsorption on the β-SiC(100) surface, two possible sites, namely the bridge site and the fourfold site (see Fig. 1), are considered. All dangling bonds that point toward the bulk are saturated by pseudosilicon and pseudocarbon atoms.[24,25] The adsorbate Al is located at a height Z above the surface.

The optimized adsorption height Z_0 is obtained by minimizing the total energy of the cluster. Although the clean β-SiC(100) surface is reconstructed, calculations show that the chemisorption energy of Al on the (2×1) reconstructed (100) surfaces is smaller than that on the ideal (100) surfaces. This implies that, after Al deposition the substrate returns to the ideal (1×1) surface from the (2×1) reconstructed one, in agreement with experiment.[13] Therefore, only the ideal (1×1) surfaces are considered.

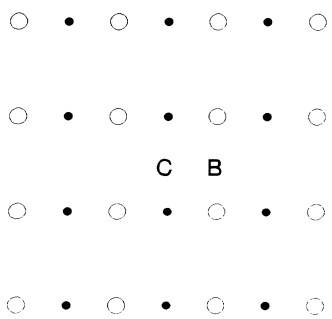

FIG. 1. Illustration of the adsorption sites. Circles represent surface atoms, dots the second-layer atoms. B indicates the bridge site and C the fourfold site.

The bond length L between Al and surface atoms and the chemisorption energy ΔE are listed in Table II for the adsorption on the different sites of both Si- and C-terminated surfaces.

From Table II, it is seen that the chemisorption energies of Al on the bridge site of Si- and C-terminated (100) surfaces are larger than that on the fourfold site, especially for the C-terminated one. Aluminum preferentially adsorbs on the bridge site and the fourfold-site adsorption is metastable. In addition, no adsorption site can be found below the surface for both Si- and C-terminated surfaces, which indicates that the Al-Si or Al-C interaction is confined to a narrow region at the interface, and interdiffusion is difficult at low temperature. These results are in qualitative agreement with experimental observations.[13]

The Al-Si bond length is much larger than the sum of covalent radii of Al and Si which means that the interaction between Al and Si does not have strong covalent character. For the Al adsorption on the fourfold site of the C-terminated (100) surface, the Al-C bond length is also larger than the sum of their covalent radii. But, in the case of bridge site adsorption, this bond length is very close to the sum of their covalent radii. The angle between the Al-C bonds is 113.8°, which is very close to the bond angle of sp^2 hybridization. Thus, the Al atom at the bridge site of the C-terminated (100) surface is sp^2 hybridized, and can be bonded with dangling bonds of the nearest C neighbors, leaving an Al dangling bond normal to the surface.

Electronic structures of Al on β-SiC(100) are calculated only for the bridge site. The total density of states (TDOS) of the system and the local density of states (LDOS) of the adatom Al are plotted in Figs. 2 and 3 together with the TDOS of the clean substrate. Vertical lines in the figures indicate the Fermi level for both the clean Si- and C-terminated (100) surface, the peak near the E_F indicated by S_1 is the surface state, which is an intrinsic empty surface state at about −8.0 eV contributed by the dangling bonds of surface atoms. Wave-function analysis reveals that the peak lying below the Fermi level (S_2) is mainly of carbon 2p character. Peaks in the range from −13.0 to −9.5 eV are mainly of Si 3p character, with some C 2p character. Comparing the TDOS of the adsorbed substrate and the clean substrate, it can be seen that the change in TDOS can be neglected in the lower-energy region. Only a slight change in TDOS is found around the Fermi level. The 3p states of Al interact with the 2p states of surface C atoms, and the 3s state of Al interacts with both Si and C atoms. In the case of the C-terminated surface, due to the hybridization of empty surface states with the 3p states of the adatom Al, part

TABLE II. The optimized bond length L (Å) and chemisorption energy ΔE (eV).

	Si terminated		C terminated	
	Bridge	Fourfold	Bridge	Fourfold
L	2.79	3.35	1.84	2.42
ΔE	−1.42	−1.27	−2.48	−1.97

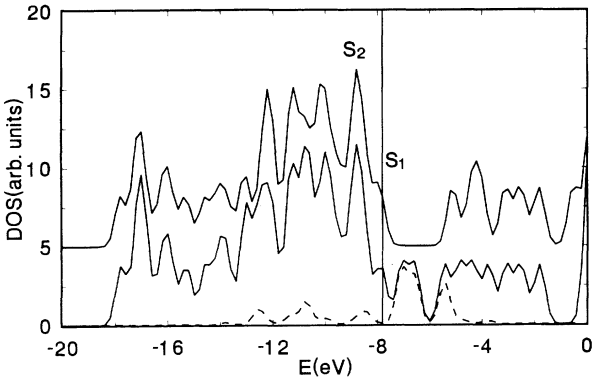

FIG. 2. The DOS for Al adsorption on the bridge site of the Si-terminated (100) surface. The upper solid line is the TDOS of the ideal surface, the lower solid line is the TDOS of the adsorbed system, and the dashed line is the LDOS of the adsorbate.

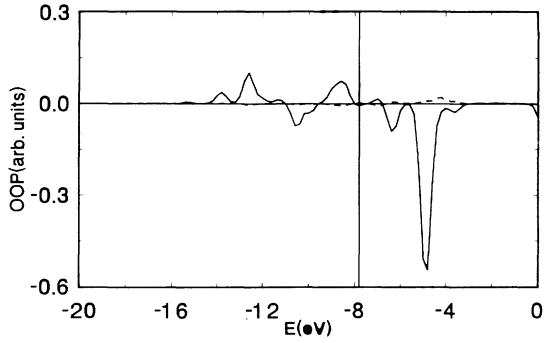

FIG. 4. OOP curves for Al adsorption on the Si-terminated (100) surface. The solid line describes the Al-Si bond and the dashed line the Al-C bond.

of the surface states shifts upwards to a higher energy in the band gap and the other part shifts downwards to the valence band.

Calculations show that, after chemisorption, a charge transfer occurs from the adatom Al to the substrate for both the Si- and C-terminated surfaces. The amount of charge transfer is about 0.53 electron on the C-terminated surface, and 0.17 electron on the Si-terminated surface, which implies that the Al-C interaction is stronger than the Al-Si interaction.

The orbital-overlap population (OOP) is of great importance in understanding the nature of bonding and is also helpful in the analysis of chemisorption. The OOP between two atoms μ and ν at energy E_i is defined as[26]

$$\mathcal{P}_{\mu\nu}^{\mathrm{OOP}}(E_i)=2\sum_{j,k} C_{ij}C_{ik}S_{jk} \ , \tag{5}$$

where j and k run over all valence orbitals of the atoms μ and ν, respectively. C_{ij} and C_{ik} are eigenvectors and S_{jk} is the overlap integral between the two atomic orbitals j and k and is always positive. The OOP is positive (bonding) if C_{ij} and C_{ik} are of the same sign and negative (antibonding) if C_{ij} and C_{ik} are of opposite sign. Similar to what is usually done to the DOS curve, the OOP is also broadened with a Gaussian of 0.3-eV width.

The OOP between the adsorbate and the first two layers versus energy curves are presented in Figs. 4 and 5 for Al adsorption on Si- and C-terminated (100) surfaces. Solid lines describe the OOP of the Al-Si bonds; dashed lines, that of the Al-C bonds. From Figs. 4 and 5, it is obvious that the interaction between the Al adatom and the host atoms in the second layer is quite weak. In the case of the Si-terminated surface, the OOP curve of the Al-Si bond has both positive and negative peaks below the Fermi level. Therefore, it can be concluded that bonding and antibonding are both responsible for the Al-Si interaction. In the case of the C-terminated surface, the OOP curve of the Al-C bond has only positive peaks below the Fermi level, which means that the interaction between the adatom Al and the surface C atom is of bonding character. These results indicate that the Al-C interaction on the C-terminated surface is stronger than the Al-Si interaction on the Si-terminated surface. The chemisorption energy and the bond order also follow the

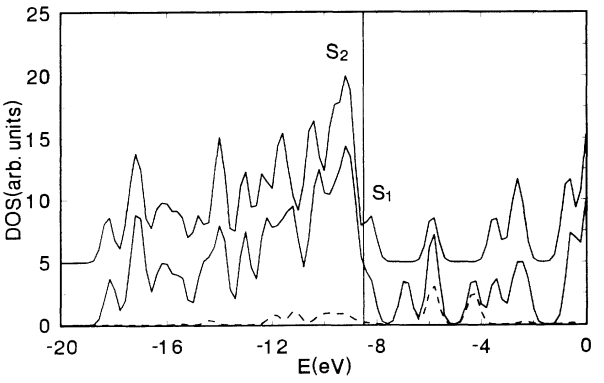

FIG. 3. The DOS for the Al adsorption on the bridge site of the C-terminated (100) surface. The other illustration is the same as that in Fig. 2.

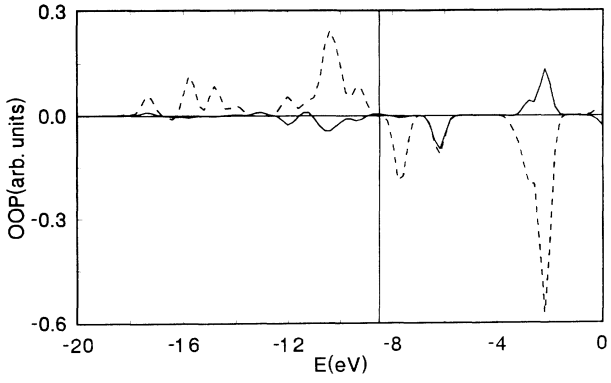

FIG. 5. OOP curves for Al adsorption on the C-terminated (100) surface. The solid line describes the Al-Si bond and dashed line the Al-C bond.

TABLE III. Bond orders of Al-Si, Al-C, and Si-C bonds for Al adsorption. The values in parentheses are the BO's of the Si-C bond before adsorption.

Bonds	Si terminated	C terminated
Al-Si	0.34	−0.09
Al-C	−0.03	0.90
Si-C	0.44 (0.45)	0.53 (0.60)

same trend.

The integral of the DOS up to the Fermi level gives the total number of electrons, and the integral of the OOP up to the Fermi level gives the total overlap population between atoms μ and ν, which is defined as the bond order (BO):

$$n_{\mu\nu}^{\mathrm{BO}}=\sum_i \mathcal{P}_{\mu\nu}^{\mathrm{OOP}}(E_i)n_i/2\ , \tag{6}$$

where n_i is the occupation number of energy level E_i.

The bond orders of Al-Si, Al-C, and Si-C bonds are listed in Table III. For both the Si- and C-terminated surfaces, the interactions between Al and second-layer atoms are very weak and have some antibonding character. The interactions between Al and surface atoms have mostly bonding character. The Al-C interaction is stronger than the Al-Si interaction. From the change in the Si-C bond order due to adsorption, it is seen that Al adsorption on the Si-terminated (100) surface hardly affects the Si-C bond, whereas Al adsorption on the C-terminated (100) surface weakens the Si-C bond. In the latter case, the bond order decreases by about 0.07 with respect to that of the clean surface.

B. Higher-coverage adsorption

For higher-coverage adsorption, a slab of ten layers, consisting of alternate silicon and carbon layers, is used to model the (100) surface of β-SiC. In this slab, one surface is Si terminated and the other is C terminated. A monolayer (coverage $\Theta=1.0$) and half a monolayer

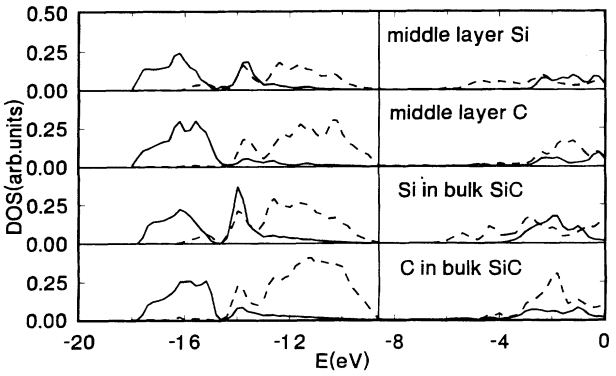

FIG. 6. The LDOS of the middle-layer Si and C atoms in a slab (upper two sections) and that of Si and C atoms in bulk SiC (lower two sections). The solid lines represent the s state and dashed lines the p state.

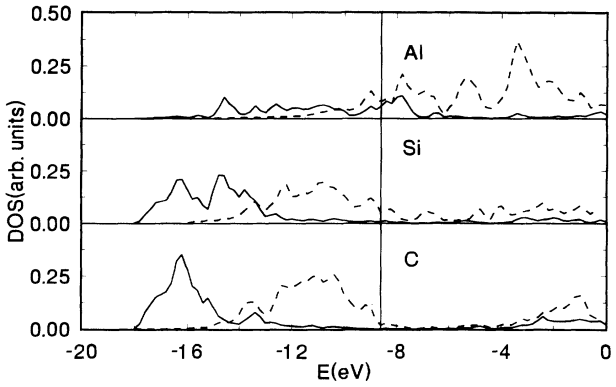

FIG. 7. The LDOS of adlayer Al atom, surface Si atom, and second-layer C atom for Al adsorption on the Si-terminated (100) surface. The Al coverage $\Theta=1.0$. Solid lines represent the s state and dashed lines the p states.

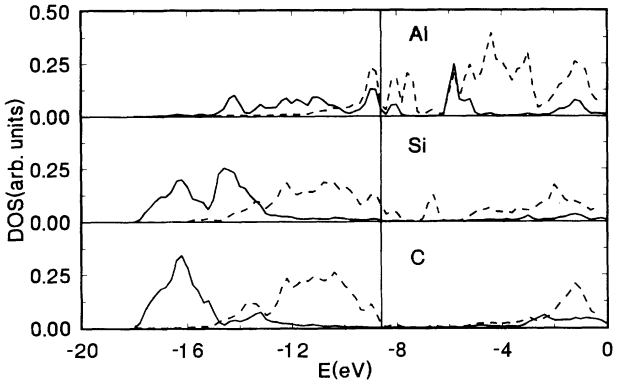

FIG. 8. The LDOS of adlayer Al atom, surface Si atom, and second-layer C atom from Al adsorption on the Si-terminated (100) surface. The Al coverage $\Theta=0.5$. Solid lines represent the s state and dashed lines the p states.

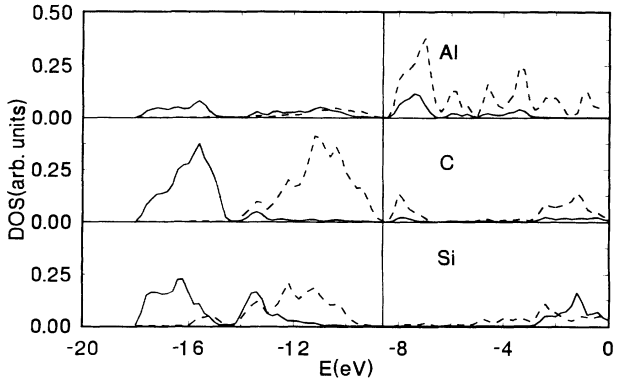

FIG. 9. The LDOS of adlayer Al atom, surface C atom, and second-layer Si atom for Al adsorption on the C-terminated (100) surface. The Al coverage $\Theta=1.0$. Solid lines represent the s state and dashed lines the p state.

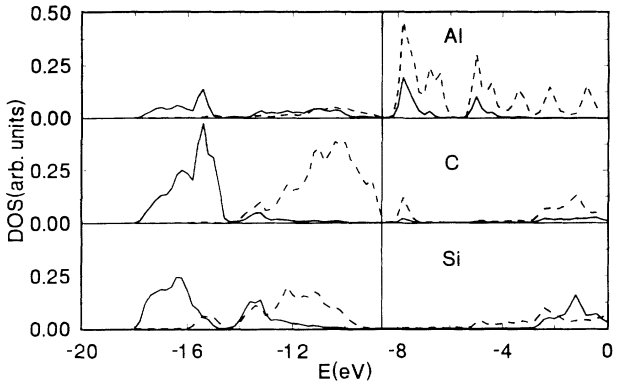

FIG. 10. The LDOS of adlayer Al atom, surface C atom, and second-layer Si atom for Al adsorption on the C-terminated (100) surface. The Al coverage $\Theta=0.5$. Solid lines represent the s state and dashed lines the p states.

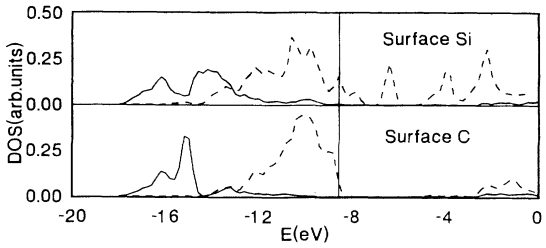

FIG. 11. The LDOS of clean surface Si and C atoms. The solid lines represent the s state and the dashed lines the p states.

($\Theta=0.5$) with each Al adatom occupying a bridge site at height Z_0 are considered. The former is the 1×1 adlayer and the latter the (2×1) adlayer. The height Z_0 was determined in the cluster calculation of the previous section.

The LDOS of Si and C in the middle layers of the slab are very similar to that of the bulk SiC (see Fig. 6). Hence, a slab ten layers thick is sufficient to describe the (100) surface. For the Si-terminated surface, the LDOS of the adatom Al and the host atoms Si and C near the surface are plotted in Figs. 7 and 8 for $\Theta=0.5$ and $\Theta=1.0$, respectively. Figures 9 and 10 are for the C-terminated surface. The vertical lines mark the top of the valence band. The LDOS of the clean surface Si and C atoms are plotted in Fig. 11 for comparison with the clean surface.

For the Si-terminated surface, the surface state in the band gap does not have any significant change either for monolayer or for half-monolayer adsorption. The sp^2-hybridized state of Al interacts with the Si($3p$) state. With increasing Al coverage (from $\Theta=0.5$ to 1.0), a part of the $2p$ state of carbon in the second layer is pushed from the valence band into the band gap (the band tail near the valence-band maximum in the lowest section of Fig. 7), and the Al-C interaction becomes stronger.

For the C-terminated surface, the sp^2-hybridized state of Al only interacts with the surface C atom; the interaction between Si and Al can then be neglected. Due to the strong Al-C interaction, an adsorption-induced surface state appears in the band gap. The intensity of this state increases with increasing Al coverage.

By comparing the LDOS of Al on Si- and C-terminated surfaces, it can be seen that the $3p$ states of Al are partially filled during the adsorption of Al on the Si-terminated surface, whereas they almost are totally unoccupied for adsorption of Al on the C-terminated surface.

C. Comparison with experiment

It has been reported in experimental studies[13] on the Al/β-SiC(100) interface that this interface is relatively sharp, and that there is no evidence for pronounced interdiffusion between Si (or C) and Al, either during deposition of films up to 75 Å thick on a room-temperature substrate, or during annealing of a 9-Å-thick film up to 1050 °C. Our calculations show that it is difficult for an Al adatom to penetrate the surface of SiC through either a Si- or a C-terminated (100) surface, which supports the above experimental finding. In the present study, although only adsorption of a single atom or a monolayer of atoms was considered, the weakening of the Si-C bond induced by Al adsorption on the C-terminated surface has been shown to be significant, which agrees quite well with the experimental observation of the formation of Al carbide,[14] since the Si-C bonds must be broken during the formation of this carbide.

Furthermore, experimental studies[13] suggest that the first two or three layers of Al do not exhibit macroscopic metallic behavior. Our calculations show that the Al-C interaction becomes stronger with increasing Al coverage. Therefore, the fact that the films display no metallic characters at two- or three-monolayer coverage may be due to the strong Al-C interaction and the formation of Al carbide. Moreover, the unoccupied $3p$ states of the Al adatom on the C-terminated surface also favor the display of nonmetallic character.

IV. CONCLUSION

By using the semiempirical charge self-consistent EHT method, low-Al-coverage adsorption on β-SiC(100) surfaces has been investigated. It was found that the bridge site was preferable for Al adsorption on either a Si- or a C-terminated surface. The interface between Al and SiC is very sharp and the interaction is only limited to a narrow region. The Al-C interaction is stronger than the Al-Si interaction, although our earlier calculation for Au adsorption on the β-SiC(111) surface[17] showed the opposite behavior.

We have also studied a monolayer and half a monolayer of Al adsorption by means of an EHT band calculation. The Al-C interaction becomes stronger with increasing Al coverage. The other properties studied are consistent with results of the cluster calculation.

*Mailing address.

[1]H. Daimon, M. Yamanaka, E. Sakuma, S. Misawa, and S. Yoshida, Jpn. J. Appl. Phys. **25**, L592 (1986).
[2]K. Yasuda, T. Hayakawa, and M. Saji, IEEE Trans. Electron Dev. **ED-34**, 2002 (1987).
[3]L. Porte, J. Appl. Phys. **60**, 635 (1986).
[4]Y. Mizokawa, K. M. Geib, and C. W. Wilmsen, J. Vac. Sci. Technol. A **4**, 1696 (1986).
[5]T. M. Parrill and Y. W. Chung, J. Vac. Sci. Technol. A **6**, 1598 (1988).
[6]R. Kaplan, P. H. Klein, and A. Addamiano, J. Appl. Phys. **58**, 321 (1984).
[7]K. M. Geib, C. W. Wilmsen, J. E. Mahan, and M. C. Bost, J. Appl. Phys. **61**, 5299 (1987).
[8]C. S. Pai, C. M. Hanson, and S. S. Lau, J. Appl. Phys. **57**, 618 (1985).
[9]I. Ohdomari, S. Sha, H. Aochi, T. Chikyow, and S. Suzuki, J. Appl. Phys. **62**, 3747 (1987).
[10]V. M. Bermudez, Appl. Surf. Sci. **17**, 12 (1983).
[11]S. Hasegawa, S. Nakamura, N. Kawamoto, H. Bishibe, and Y. Mizokawa, Surf. Sci. **206**, L851 (1988).
[12]M. A. Taubenblatt and C. R. Helms, J. Appl. Phys. **59**, 1992 (1986).
[13]V. M. Bermudez, J. Appl. Phys. **63**, 4951 (1988).
[14]V. M. Bermudez, Appl. Phys. Lett. **42**, 70 (1983).
[15]S. P. Mahandru and A. B. Anderson, Surf. Sci. **245**, 333 (1991).
[16]A. B. Anderson and C. Ravimohan, Phys. Rev. B **38**, 974 (1988).
[17]Xie Xide, Zhang Kaiming, and Ye Ling, Commun. Theor. Phys. **1**, 131 (1982).
[18]Lu Wenchang, Ye Ling, and Zhang Kaiming, Chinese Phys. Lett. **9**, 101 (1992).
[19]Lu Wenchang, Yang Weidong, and Zhang Kaiming, J. Phys. Condens. Matter **3**, 9079 (1991).
[20]H. Hoechst, M. Tang, B. C. Johnson, J. M. Meese, G. W. Zajac, and T. H. Fleisch, J. Vac. Sci. Technol. A **5**, 1640 (1987).
[21]A. R. Lubinsky, D. E. Ellis, and G. S. Painter, Phys. Rev. B **11**, 1537 (1975).
[22]E. Clementi and D. L. Raimondi, J. Chem. Phys. **38**, 2686 (1963).
[23]W. Lotz, J. Opt. Soc. Am. **60**, 206 (1970).
[24]W. A. Goddard, J. J. Barton, A. Redondo, and T. C. McGill, J. Vac. Sci. Technol. **15**, 1274 (1978).
[25]Zhang Kaiming and Ye Ling, Acta Phys. Sinica **29**, 686 (1980) (in Chinese).
[26]R. Hoffmann, Rev. Mod. Phys. **60**, 601 (1988).